International Journal of Engineering Trends and Technology
ISSN: 2231–5381 / https://doi.org/10.14445/22315381/IJETT-V73I6P118

Volume 73 Issue 6, 214-224, June 2025

Original Article

Experimental Diagnosis of Eccentricity Faults in a Dynamic Gear System Using Model-Based Approaches

Yakeu Happi Kemajou Herbert[1], Tchomeni Kouejou Bernard Xavier[2], Alfayo Anyika Alugongo[3]

[1,2,3]*Vaal University of Technology, Department of Industrial Engineering, Operation Management and Mechanical Engineering, South Africa.*

[1]*Corresponding Author : kemajouy@vut.ac.za*

Received: 18 December 2024 Revised: 03 April 2025 Accepted: 10 June 2025 Published: 28 June 2025

Abstract - *In this paper, an experimental study was conducted on a gear mechanism with eccentricity anomalies, emphasising advanced time-frequency domain methods to improve the diagnosis. Vibrations captured under various operating conditions were examined using RPM-frequency mapping, Short-Time Fourier transform (STFT), 3D waterfall FFT, and 3D Time-Frequency analysis. These techniques allowed for more accurate detection of eccentricity signs, including its impact on the interaction between gears and transmission performance. The results showed that elaborate phenomena such as intense modulation and nonlinear behaviors complicate accurate fault detection using traditional methods based solely on time and frequency domain. However, the multidimensional method adopted here allows for highlighting localised signal indicators that are directly associated with transmission disturbances due to eccentricity. This work, therefore, highlights the need to apply time-frequency methods to monitor the condition of gears and optimize their maintenance more effectively.*

Keywords - *Eccentricity fault, Gear mesh stiffness, RPM-frequency map – STFT, 3D time frequency, Transmission error, Two-stage spur gear system, 3D waterfall FFT.*

1. Introduction

Gearboxes are critically important in various fields, such as aeronautics, industrial production, and wind power generation. An eccentricity defect in the gearboxes can lead to irregular power transmission, torque fluctuations, and consequently reduced energy efficiency. It is, therefore, essential to identify these irregularities quickly to avoid costly malfunctions and ensure reliable operation. During use, these anomalies produce vibrations affecting the device's overall performance. They also cause accelerated wear of delicate components such as gear teeth and bearings. These vibrations change as the problems deteriorate, making them an essential indicator to observe [1]. Numerous studies have concentrated on analyzing torsional and lateral vibrations to address this by developing numerical models to understand gear dynamics better. To more effectively understand and predict these phenomena, various studies have focused on the study of lateral or torsional vibrations using advanced numerical models. For example, Wang and his group [2] used the finite element technique (FE) to refine detection parameters and improve the identification of defects associated with eccentricity. The properties of these defects have been studied both theoretically and experimentally. This now makes it possible to evaluate better elements, such as the interaction between variables and the evolution of the transmission error (TE), which is essential information for correcting these errors and improving the performance of mechanical systems. Zhou et al. [3] calculated the time-variable mesh stiffness for spur gears and studied the impact of gear eccentricity errors on mesh stiffness. Additionally, a planetary gear train's dynamic model was created to assess gear eccentricity's effects on mesh stiffness and overall dynamic performance [4]. To investigate the effects of time fluctuation of the pressure angle and gear backlash on spur gear structures, Yi et al. [5] suggested a nonlinear dynamic model. Suxiang et al. [6] proposed a design idea with a novel transmission mechanism for an eccentric modified gear to ensure a variation of gear tooth backlash within the permissible range. Methods for calculating TE resulting from eccentricity errors in gear trains were initially proposed by Sun [7] and Michalec. Following this, Bo [8] and Wu [9] provided their calculations after studying the effects of single-gear eccentricity errors on TE. Ottewill [10] used experimental tests to estimate the TE of a pair of gears with eccentricity errors and demonstrated how different levels of TE and backlash corresponded to various phases of eccentricity errors. Rocca [11] used the TE spectrogram and represented TE as a trigonometric function to determine the eccentricity error of the helical gear mechanism. Furthermore, Gu [2] developed a mathematical model to simulate eccentricity's impacts on planetary gears' quasi-static and dynamic behavior. In another research [11], finite element models were used to examine the impact of eccentricity errors

on the performance of spur and helical gears. Aijun et al. [12] investigated a multi-stage planetary transmission system's mathematical model to study gears' dynamic response affected by profile defects and assembly errors, which subsequently caused crack-like failures. Time-series imaging and FFT spectrum methods were used to analyze the dynamic response. Liu et al. [13] proposed a new dynamic model to study the combined effect of eccentricity and wear using the technique of tooth contact under load, aiming to better understand the meshing behavior under these circumstances.

Despite numerous models being developed and researched in the literature, precise calculations of TE resulting from eccentricity errors are rare. Additionally, many experimental investigations do not focus on the impact of eccentricity errors on TE. Under real experimental conditions, the TE, mainly caused by eccentricity, is rarely quantified by current models. For an accurate analysis of the non-linear dynamic behaviour of the gear system, it is important to provide a detailed analytical model that can reveal the meshing relations and specific nonlinear properties. Fourier analysis techniques are considered more effective in diagnosing gear deterioration than the time method and frequency approach. When the vibration signal is transient, faults are effectively characterised by complex spectral variations.

In machine diagnostics, time-frequency analysis is a valuable tool for reflecting the vibration signal more accurately than previous methods, as it provides more information about the signal in frequency and time. Identifying appropriate analytical methods and methodologies for problem identification is essential for studying failure diagnosis mechanisms. In this study, an effective analysis technique is used to identify anomalies associated with eccentricity effectively and the impact of eccentricity defects on a two-stage spur gear system is analysed in depth, with particular attention to how eccentricity parameters and time-varying mesh stiffness influence the system vibration characteristics. Various sophisticated tools such as RPM frequency mapping, 3D waterfall FFT (Fourier fast transform), and short-time Fourier transform (STFT) are used to examine vibration signals and identify potential irregularities. The combined use of these time-frequency analysis methods and RPM mapping facilitates the early detection of signs of eccentricity in the spur gear system.

To understand the impacts of this type of anomaly, several operational scenarios were modelled to examine how eccentricity affects the system's lateral, torsional, and dynamic behaviours. The article is organized as follows: Section 2 details the two-stage spur transition model. Section 3 describes the design and installation of the test bench. Section 4 highlights the primary analysis. The effects of pitch eccentricity on vibration and transmission errors are analysed using different analysis techniques, such as RPM-frequency map, 3D waterfall FFT, and STFT, to more accurately identify anomalies associated with eccentricity. Section 5 draws a comparative discussion between these time-frequency analysis techniques and traditional analysis. Finally, Section 6 summarizes the key lessons learned from the study.

2. Spur Gear System Model

Figure 1 shows a two-stage gear system without considering the pinion backlash and inter-tooth friction. Subsequently, the gears are viewed as solid cylinders connected by a meshing stiffness, representing the elastic coupling between the teeth given the absence of inter-tooth friction in the pinion and gear. The parameters of the two-stage gear system are listed in Table 1.

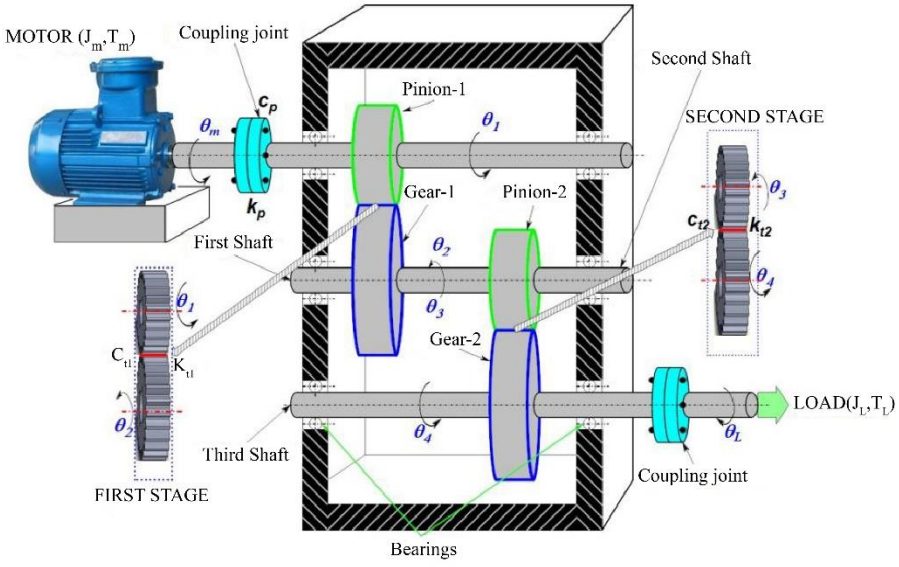

Fig. 1 Dynamic model of a gear system with two stages

Table 1. The two-stage gear under study physical characteristics

Specifications	Stage 1	Stage 2
Young Module (E)	2068×10^{11} Pa	2068×10^{12} Pa
Number of teeth	$Z_1 = 30$ & $Z_2 = 90$	$Z_3 = 30$ & $Z_4 = 90$
Poisson's ratio	3×10^{-1}	3×10^{-1}
Angle of pressure	20 degrees	20 degrees
Pinion & gear base circle radius (mm)	$R_1 = 30.1$ & $R_2 = 76.1$	$R_3 = 30.1$ & $R_4 = 76.1$
Mass (kg)	$M_1 = 0.96$ & $M_2 = 2.88$	$M_3 = 0.96$ & $M_4 = 2.88$
Bearings meshing stiffness (Ns/m)	$k_1 = k_3 = 656\times10^8$	$k_2 = k_4 = 656\times10^8$
Bearings damping coefficient (Ns/m)	$c_1 = c_2 = 18\times10^6$	$c_3 = c_4 = 18\times10^6$
Coupling torsional stiffness (Ns/m)	$k_p = 44\times10^5$	$k_g = 44\times10^5$
Coupling damping coefficient (Nms/rad)	$c_p = 5\times10^5$	$c_g = 5\times10^5$

3. Set-Up Gear System Description

The two-stage spur gear arrangement used in the experimental test rig was designed to mimic a real-world gear transmission system. A flexible coupling drives a gear train via an electric motor, as shown in Figure 2. Using a digital speed controller, the input shaft rotates at a constant speed of 1,500 rpm.

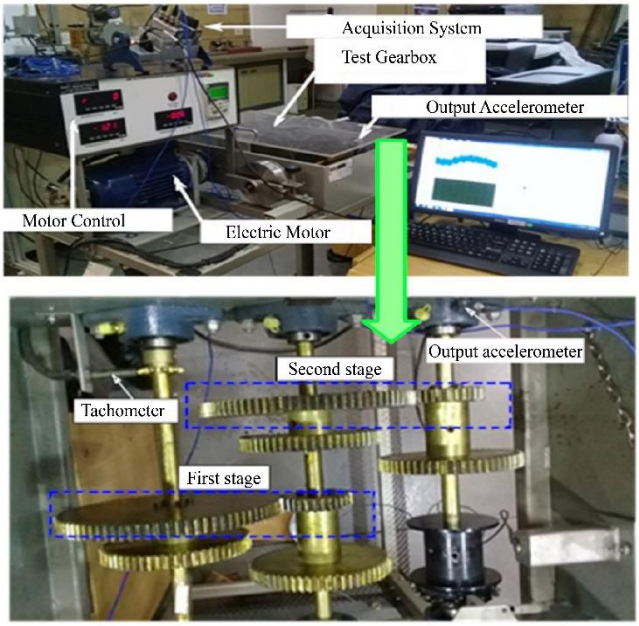

Fig. 2 Experimental gearbox testing apparatus

To better understand the lateral rotational reactions of the system, piezoelectric sensors were used to record vibrations. With a sensitivity of 10.2 mV/m/s2 and capable of detecting frequencies up to 150 kHz, these accelerometers were carefully mounted on the reduction and support bearings, as shown in Figure 3.

Data were collected at high speed, at a sampling rate of 15 kHz, using an acquisition system integrated with NI LabVIEW. Programs developed with MATLAB were then used for signal analysis: Time-frequency transformations were used to isolate the major vibration characteristics.

Three configurations were used to test the system:

- Healthy gear system (no eccentricity),
- Moderate defect (50 µm eccentricity),
- Significant defect (100 µm eccentricity).

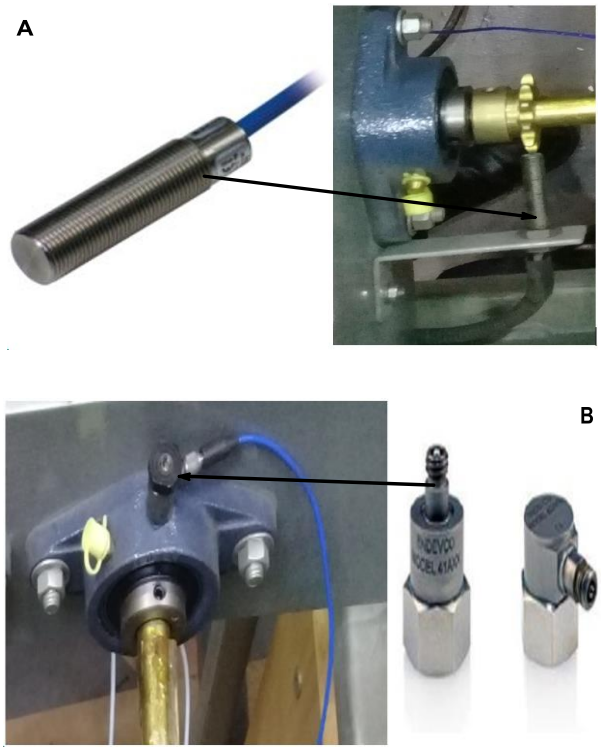

Fig. 3 (A) Speed sensor, and (B) Accelerometers.

The gear pair under consideration consists of steel spur gears with 30 and 90 teeth per stage. Dial indicators and high-resolution coordinate measuring instruments were used to confirm that the geometric centre of the pinion had been displaced by 50 µm and 100 µm using precision machining and alignment tools to create eccentricity.

Each configuration was tested multiple times to ensure consistency, and isolating mounting and shielding strategies were used to reduce noise.

4. Results

4.1. Gearbox Vibration Experimental Results

The experimental test rig is depicted in Figure 2. The acquisition system collected the experimental data and revealed the gear vibration signal as noise interference produced by a damaged gear changing over time.

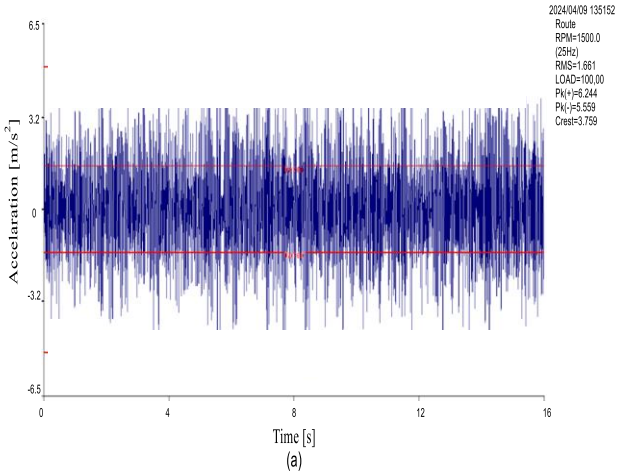

Fig. 4 Gear response in a healthy state

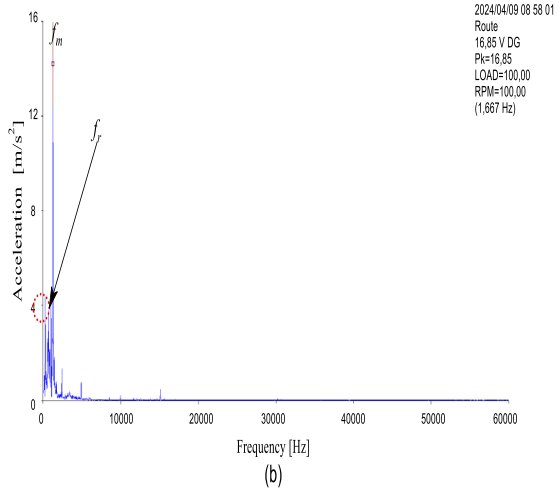

Fig. 5 Spectrum result of vibration response of healthy gear

Figure 4 shows a stable and balanced vibration signal with a uniform and symmetrical waveform around zero. This profile reflects smooth operation without significant errors or interruptions. A low and constant amplitude indicates that the system operates normally without obvious offsets or eccentricities.

The absence of perceptible vibrations indicates that all mechanical components are well-adjusted and show no signs of permanent failure. The parts fit together harmoniously, and the load transfer is continuous, indicating excellent overall operating conditions.

In Figure 5, a clear peak in the mesh frequency (f_m) is observed, corresponding to the smooth passage of the gear teeth. A second, more attenuated peak occurs at the rotational speed (f_r), reflecting the main movement of the crankshaft. The spectral analysis shows great clarity: virtually no harmonics or sidebands were detected, indicating the absence of significant mechanical defects such as eccentricity. The low noise level confirms the system's stability, while interference and parasitic resonances are practically absent.

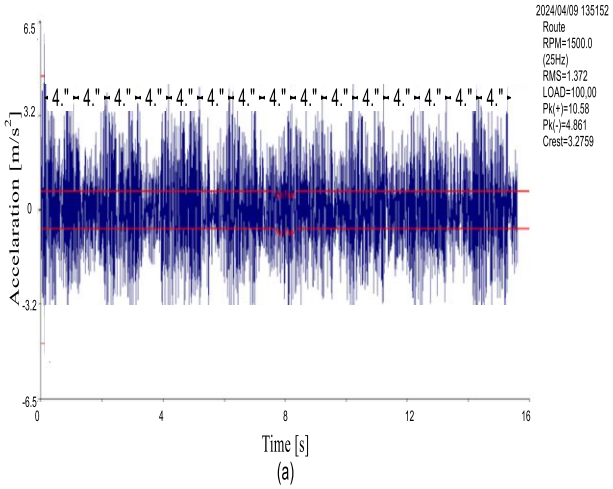

Fig. 6 Gear response with 50µm eccentricity

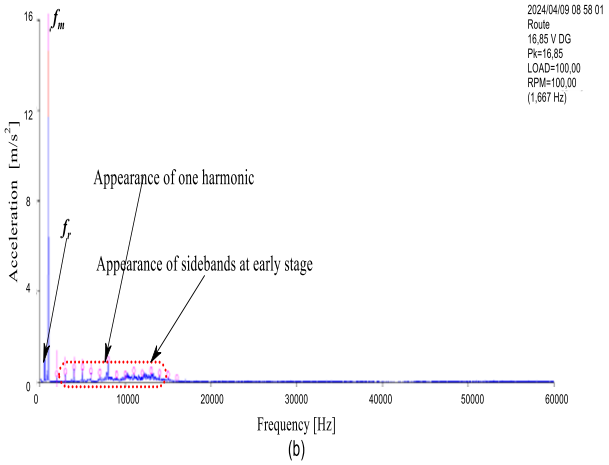

Fig. 7 Spectrum result with 50 µm eccentricity

Figure 6 shows constant oscillations with distinct peaks that reappear periodically. This indicates that the system is experiencing some periodic vibration associated with a shift in the rotation axis. Instead of regular operation, the signal shape is now irregular, suggesting that the part no longer rotates exactly on center. This anomaly influences the fit of the gear teeth, altering their stiffness with each interaction. The increase in the overall vibration level also indicates that the transmission of mechanical energy to the housing is

becoming increasingly unstable. Figure 7 shows the early appearance of bands around the fundamental frequency (f_n), indicating the first signs of an anomaly associated with eccentricity. Currently, the misalignment is moderate.

However, the system is beginning to show signs of mechanical malfunction, although the damage remains contained. From Figure 8, the signal shows uneven and high-amplitude vibration peaks, significantly higher than those detected in a system in good condition and with an eccentricity of 50 µm. The vibration envelope shows instability, indicating a nonlinear mechanical response of the system. Double peaks and areas of high vibration intensity make the signal more difficult to analyse. These elements reveal a significant breakdown in the mechanical coupling, accompanied by a rapid increase in force variations at each revolution.

An accentuated eccentricity strongly disrupts the centre of rotation, causing the appearance of unstable and irregular radial forces. To statistically estimate the amplitude variations between healthy (0 µm) and defective (50 µm and 100 µm), a uniquely significant ANOVA (Analysis of Variance) was performed on the RMS vibration amplitudes obtained in terms of 10 repetitions. Analyzing a revelation of significant deviations ($F(2,27) = 24.6$, $p < 0.001$), post-hoc Tukey tests confirmed that the pairwise comparisons (0 vs 50 µm, 0 vs 100 µm, 50 vs 100 µm) were significant ($p < 0.01$).

This confirms the visual trends in Figures 7 and 9, where the sideband energy increases with eccentricity. Therefore, studying vibrations in various situations, namely, a healthy system, an eccentricity of 50 µm, and an eccentricity of 100 µm, reveals an increase in spectral complexity and the gradual emergence of modulation effects. Table 2 provides a synthetic overview of the main vibration parameters observed during the experiments, thus facilitating the comparison and visualisation of these different situations.

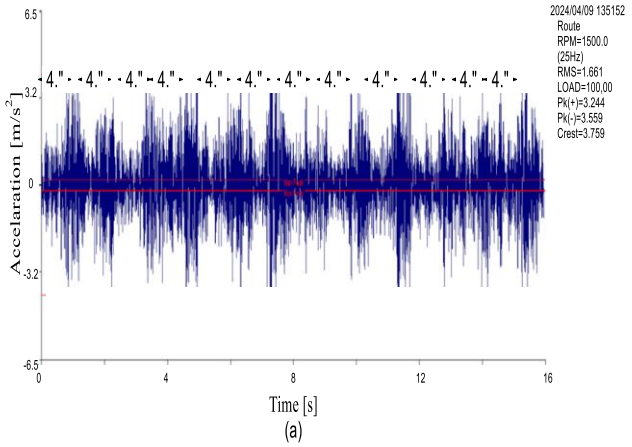

Fig. 8 Gear response with 100µm eccentricity

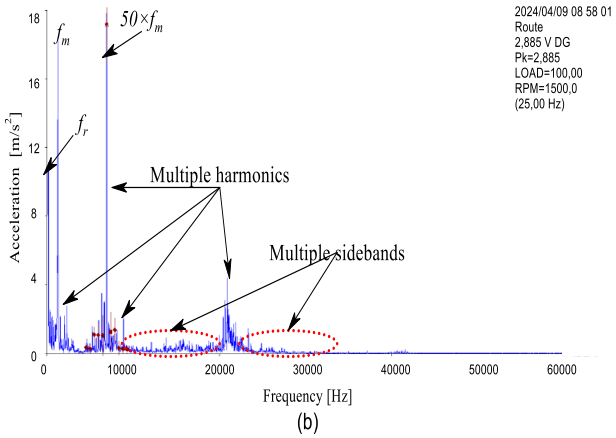

Fig. 9 Spectrum result with 100 µm eccentricity

Table 2. Vibration responses under various eccentricity conditions

Condition	Peak Amplitude (m/s²)	Dominant Frequencies (Hz)	Sidebands Present	Current Transmission Error
Perfect	0.15	Mesh frequency 2×(500–600 Hz)	None	Stable/ Minimum
Eccentricity 50 µm	0.4	Mesh frequency + sidebands (485–800 Hz)	Moderate	Moderately Increasing
Eccentricity 100 µm	0.7	Deep visible spectrum (10–20 kHz)	Severe	Unstable and Highly Significant

4.2. Extraction of Experimental Result Feature

As illustrated in Figures 5, 7, and 9, interpreting the spectra of the collected signals is not always straightforward. A mapping method that combines engine speed (RPM) and frequency data, in conjunction with the STFT, 3D waterfall FFT, and 3D Time-Frequency map, is implemented to overcome this challenge.

This method allows for separating non-stationary elements derived from the experimental test. Figure 10 presents the analysis scheme implemented on a spur gear system. Time-frequency analysis techniques are now being used to improve fault identification.

These methods enable the direct deduction of complex vibration signatures from experimental data, thus overcoming the constraints of conventional approaches. Identifying various anomalies in rotating machinery has been particularly effective for vibration analysis, combined with these time-frequency techniques.

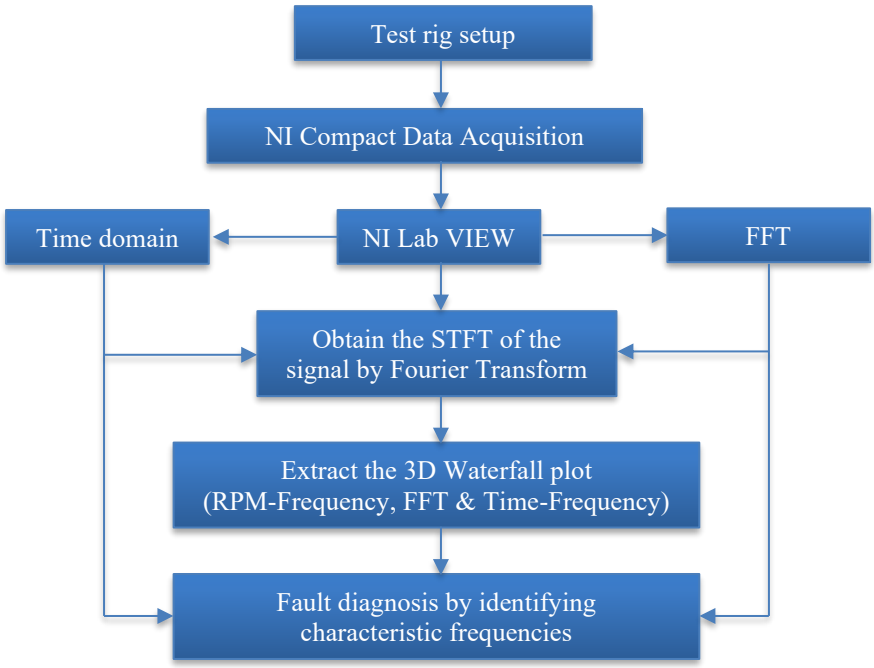

Fig. 10 Flowchart of experimental process

The STFT, one of these tools, can analyse the temporal evolution of signal frequencies through three-dimensional visualisation. In this context, the signal "s" refers to the result of applying STFT to the time sample "y" [6].

$$STFT(w,t) = \int_{-\infty}^{\infty} \bar{g}(u-t)\, f(u) e^{-2\pi t w u} du \qquad (1)$$

Where t represents the window time tracking parameter g and $\bar{g}$ is the conjugate complex of the function g (μ). The 3D frequency spectrum, with gear eccentricity as the controlling parameter, is shown in the following figures. This study examines the dynamic nonlinear properties of a spur gear system that has not and has an eccentricity defect. All other parameters remain unchanged.

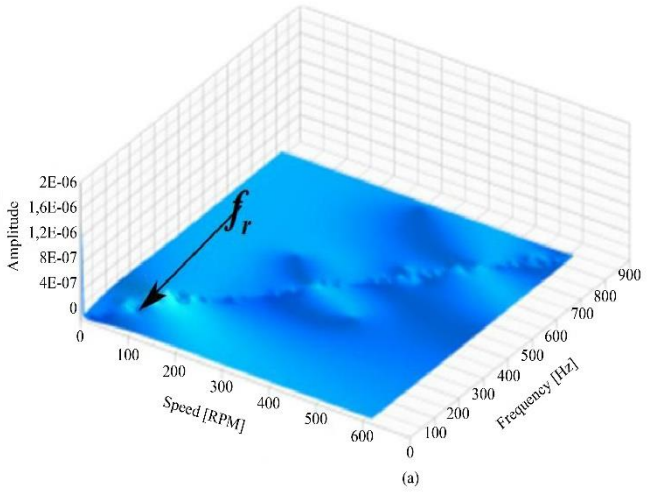

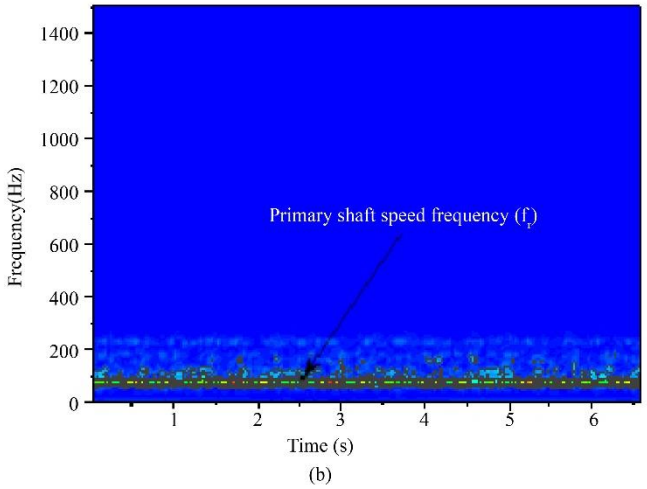

Fig. 11 STFT result of healthy gears

Figure 11(a) illustrates that the examined surface is uniform and smooth, without any notable defect marks. In a gearbox in excellent condition, the signal energy remains low to moderate, reflecting a constant and uniform performance. No sidebands or specific harmonics were observed that could indicate an irregularity associated with eccentricity. In addition, no temporary phenomena, modulations, or abnormal frequencies are observed, which attests to the mechanism's good working condition. Figure 11(b) shows that the blue diagram reflects minimal vibration activity, typical of a healthy gearbox. The constant presence of a low-frequency element (indicated by *fr*) reveals a smooth and regular operation of the gear mechanism. The absence of any disturbance, harmonic or modulation indicates that an

eccentricity defect does not influence the system. As shown in Figure 12 (a), the first signs of mechanical imbalance appear around the rotation frequency (fr) and the modulation frequency (fm). There is a significant increase in the amplitude, which is between 0.0008 m and 0.0012 m. These elevations, linked to the apparent maxima on the surface spectrogram between 0.0008 m and 0.0016 m, indicate a slight displacement of the shaft relative to its rotation axis, a precursor to the onset of eccentricity failure. For the moment, even if the vibration behavior is affected, the impacts remain quite limited.

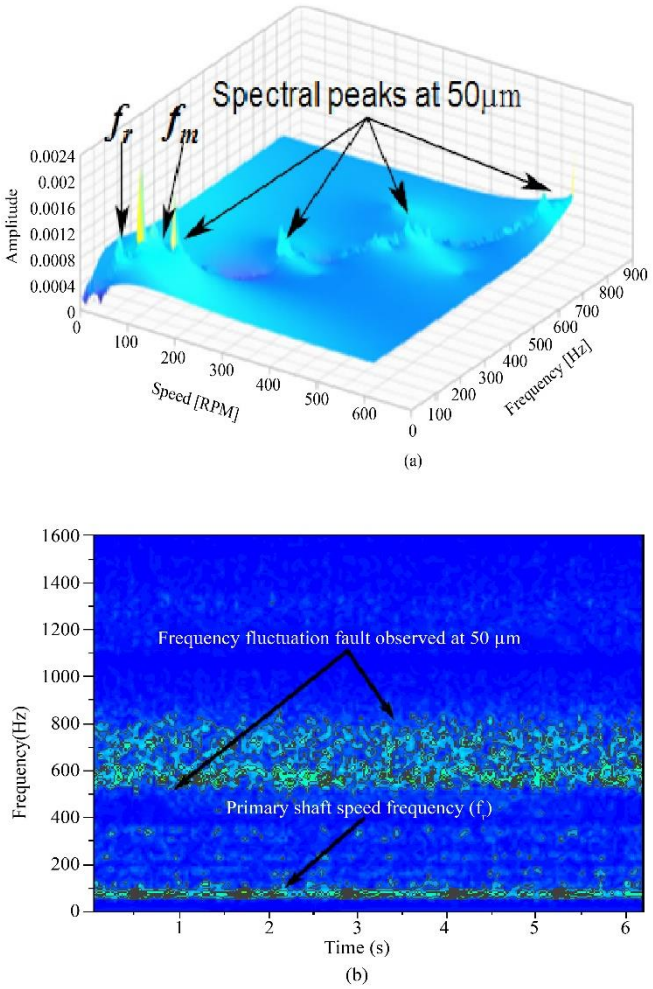

Fig. 12 Faulty gear system with 50µm eccentricity: (a) RPM-frequency result, and (b) STFT result.

In contrast, Figure 12 (b) shows a more pronounced variation in frequency between 485 Hz and 800 Hz, associated with an eccentricity of 50 micrometers. This irregularity coincides with the rotation frequency of the central axis (f_r), indicating that a simple offset, even negligible, already measurably influences the vibration dynamics of the gear system. This attests that the rotating element is no longer ideally centered, creating periodic fluctuations that the sensors can detect.

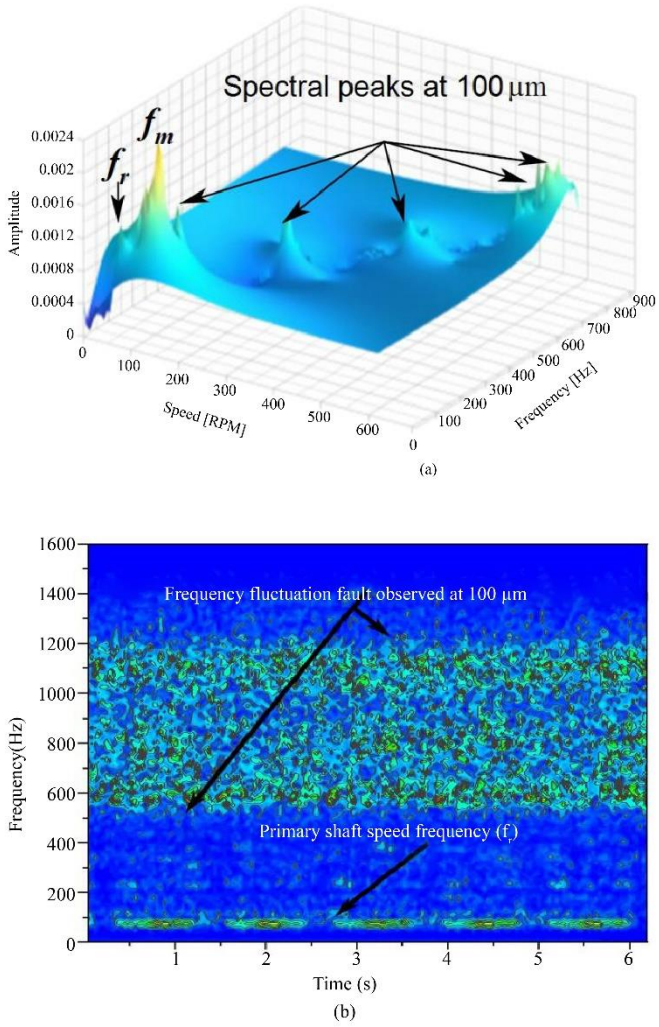

Fig. 13 Faulty gear system with 100µm eccentricity: (a) RPM-frequency result, and (b) STFT result.

As Figure 13(a) clearly shows, the situation is much more worrying. The system vibration response is more potent in amplitude and distribution in the time-frequency domain. More pronounced and regular variations around 0.0012 m and 0.002 m reveal an amplified mechanical imbalance. An increased eccentricity (100 µm) places additional demands on the gearbox elements. The rotating parts present a notable shift, observable through increased detected signal energy. Consequently, the impacts associated with gear eccentricity become more noticeable, and monitoring the evolution of the vibration peaks allows for observing the deterioration of the phenomenon.

In Figure 13(b), a significant increase in the anomaly is observed in the frequency band from 485 Hz to 1280 Hz. The frequency fluctuations are more noticeable with an eccentricity of 100 µm, indicating a marked intensification of the vibrations. This behavior directly links the increase in eccentricity and the intensity of mechanical imbalance. The

increase in eccentricity leads to an intensification of the disturbances affecting the rotation frequency of the main shaft (f_r), highlighting an increasingly marked shift in the system.

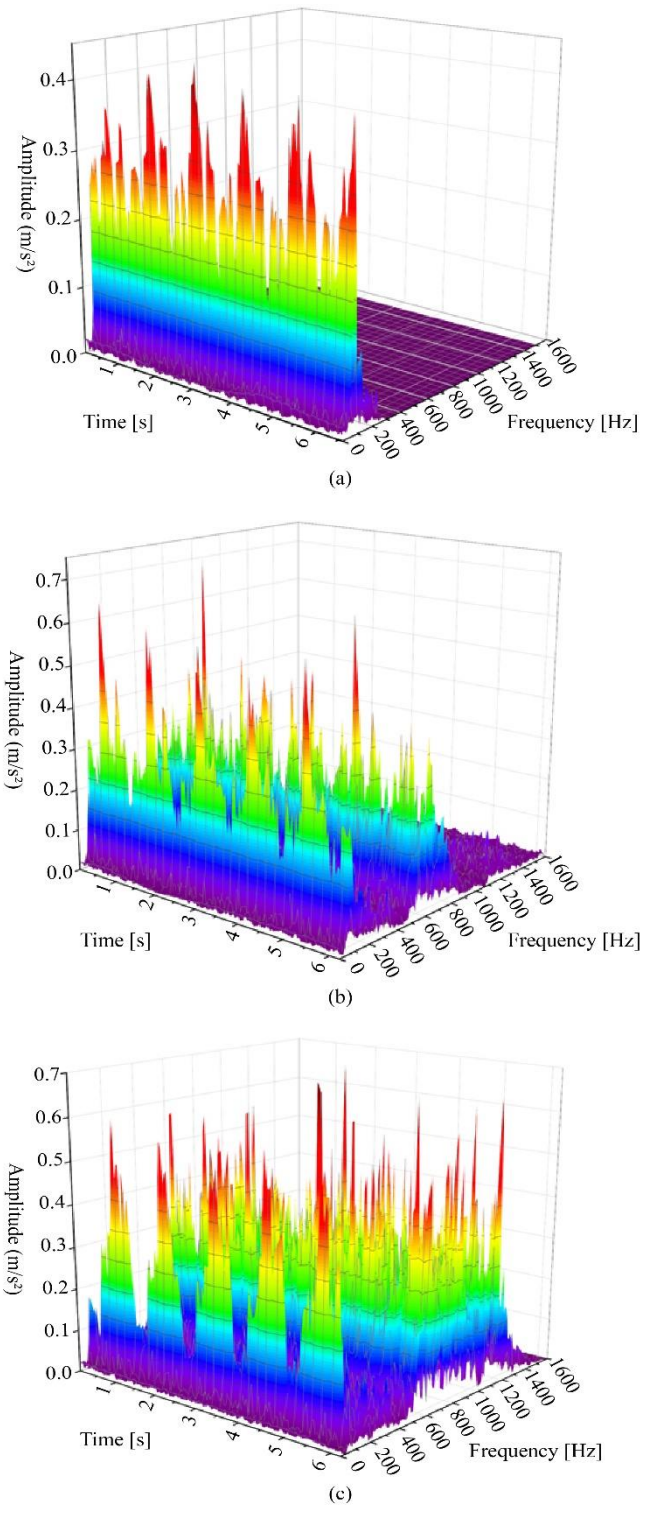

Fig. 14 3D Time-Frequency map: (a) Healthy system gear, (b) Faulty gear system with 50 µm eccentricity, and (c) Faulty gear system with 100 µm eccentricity.

Figure 14 (a) represents the vibration signal of a gearbox in perfect condition without any indication of failure. The vibration intensity is moderate and remains constant over time. The visible peaks clearly and consistently demonstrate a balanced and regular system operation. Regarding the frequencies, no anomalies are detected; they remain within the 300 to 1400 Hz range, demonstrating satisfactory dynamic stability. In contrast, Figure 14(b) reveals the first signs of anomaly with an eccentricity of 50 µm. Slight irregularities appear between 300 and 880 Hz in the vibration signature, with an amplitude reaching 0.7 m/s². These fluctuations indicate the beginning of a misalignment; the energy transmitted by the input shaft becomes less regular, and the signal's amplitude increases approximately every half-second. Figure 14(c) shows a significant deterioration of the situation, where an eccentricity of 100 µm causes much more pronounced disturbances. The defect significantly affects the gearbox's operation, with the risk of causing mechanical damage. Multiple harmonics are observed from 300 Hz to 1400 Hz, signalling a modified vibration behaviour. Unlike the previous case of an eccentricity of 50 µm, several high-frequency fluctuations are now observed, with amplitudes exceeding. To accurately identify the transmission error, a 3D FFT was used to highlight the transmission error within the gear system.

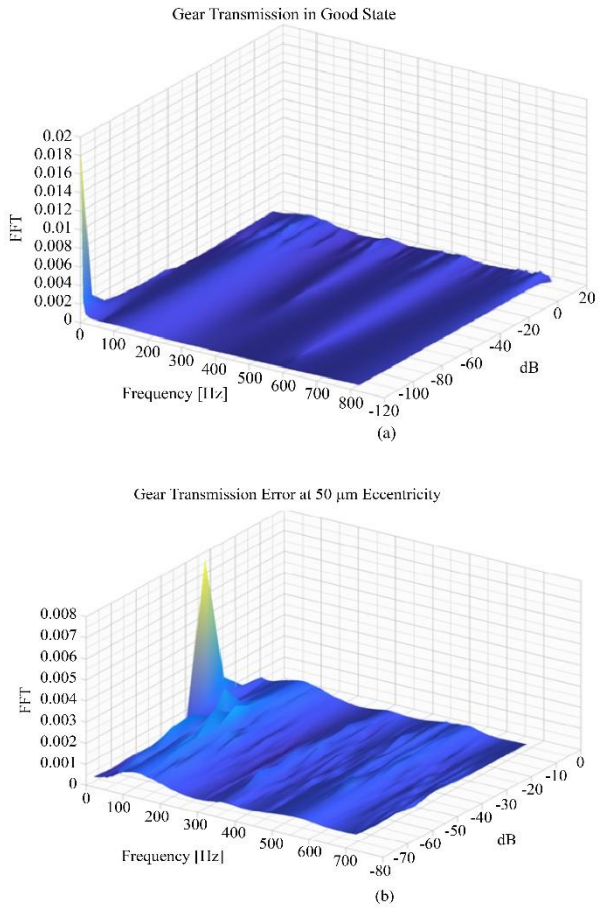

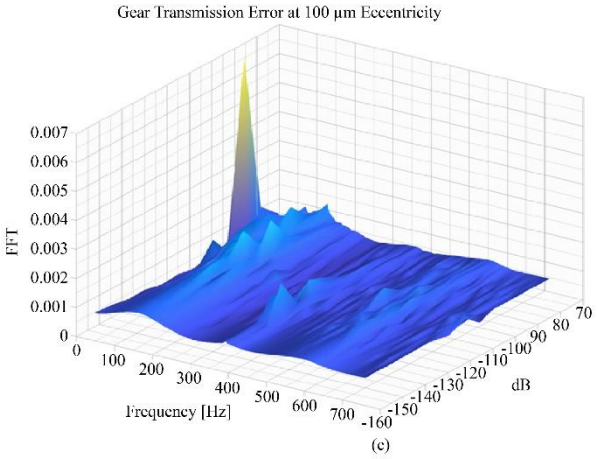

Fig. 15 3D Waterfall FFT of lateral vibration response: (a) Healthy gear system, (b) Faulty gear system with 50 µm eccentricity and (c) 100 µm eccentricity.

Figure 15(a) shows the examination of a healthy gear system by a 3D lateral vibration cascade using FFT. All frequencies from 0 to 800 Hz display reduced amplitudes in this configuration, illustrating a smooth, vibration-free transmission.

A spectrum free of sharp peaks indicates the system is properly balanced, ideally positioned, and free of mechanical defects such as eccentricity. However, Figure 15(b) shows a significant increase in the low frequencies, approximately 50 Hz. This signal reveals a voltage build-up or the beginning of an imbalance, highlighting that the system is beginning to suffer the consequences of a 50 µm eccentricity anomaly. Despite the problem being clear, the device continues to operate. Figure 15(c) illustrates a more alarming situation.

The spectrum is more spread out, with several secondary peaks. This indicates an increasingly chaotic transmission of mechanical energy. The imbalance strengthens and becomes recurrent, the vibrations intensify, and the mechanical efficiency decreases. There are also significant variations in the 100-550 Hz range, which are directly associated with the transmission error due to the 100 µm eccentricity defect. Pearson correlation coefficients were calculated to quantify the relationship between eccentricity levels (50 µm, 100 µm) and sideband energy around the thread frequency (fm ± fr). Strong positive correlations were established ($r = 0.89$, $p < 0.001$ for 50 µm; $r = 0.93$, $p < 0.001$ for 100 µm), confirming that eccentricity linearly amplifies modulation effects.

4.3. Analysis of Spur Gear System Transmission Errors

The transmission error of a two-stage gear system is analyzed under standard operating situations and with various eccentricity defects. In the healthy gear scenario, the transmission error remained stable, indicating the correct performance of the gear mechanism, as demonstrated in Figure 16.

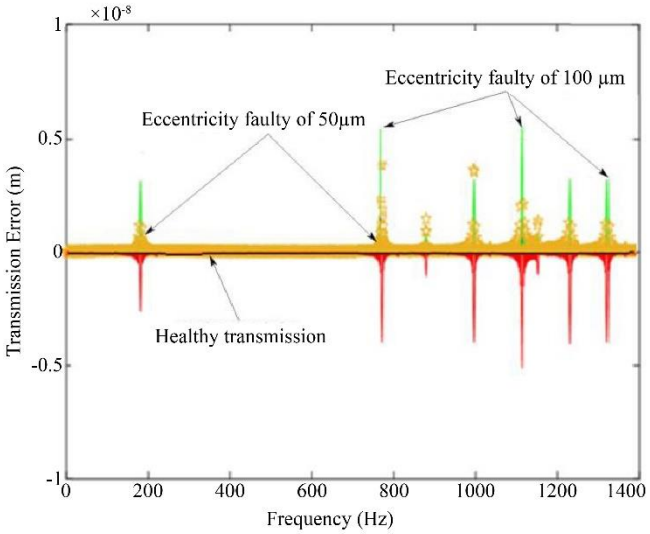

Fig. 16 2D Transmission error for health and defective gears system

As shown in Figure 16, the signal is almost non-existent and has only a slight background noise (shown in black in the center). This means the device operates balanced, without excessive pressure and movement, and the gears mesh perfectly. However, when the eccentricity increases to 50 µm, transmission error peaks appear at specific frequencies, signalling the first indicators of an imbalance in the system. Although they are not yet serious, these are the initial indications of a problem. However, at a 100 µm eccentricity, numerous error peaks in the transmission at different frequencies are observed, and the impact on the system becomes considerably more noticeable (more visible on the left of Figure 16). The energy flow becomes chaotic and inefficient. A linear regression model was fitted by estimating the TE with eccentricity values (0–100 µm). The model accounted for 85% of the TE variance ($R2 = 0.85$, $p < 0.001$), with a slope of 0.12 µm/µm (95% CI [0.10, 0.14]), indicating that TE increased by 0.12 µm per 1 µm of eccentricity. The impact of eccentricity defect is particularly evident in Figures 11, 12, 13, 14 and 15. The increase in transmission errors is due to eccentricity faults resulting from gear misalignment and a growing angular deviation between the meshing gears. The results demonstrate a significant improvement in detecting irregularities, highlighting the superior effectiveness of sophisticated methods in identifying crucial variations in vibration patterns.

5. Discussion

The experience described in the paper clearly shows that sophisticated time-frequency analysis methods, such as RPM frequency map, STFT, 3D waterfall FFT, and 3D Time-Frequency map, offer significant benefits over conventional analysis approaches such as time domain and frequency domain for identifying eccentricity anomalies in gear systems. In the time domain, the vibration signals can indicate regular

impacts and irregularities, but this data is frequently overwhelmed by noise and obscured by other dynamic elements. For instance, the results show impacts due to eccentricity (Figures 6 and 8), yet their understanding remains qualitative and imprecise without further analysis. The FFT represents the predominant frequencies but does not capture the time changes of non-stationary signals. Regarding eccentricity defects, modulations and sidebands around the mesh frequencies can be distinguished (Figures 7 and 9). However, their time progression and relationship to operational parameters, such as rotation speed, remain unclear.

However, the Frequency-RPM map establishes a link between frequencies and rotational speed (RPM), facilitating the identification of particular patterns associated with eccentricity. For instance, Figures 12(a) and 13(a) show that sharp peaks and frequency slices are explicitly linked to 50 µm and 100 µm eccentricity anomalies, respectively. This enables early identification and accurate localization of anomalies. The STFT segments the signal into small time windows before performing the FFT, making it possible to detect changes in frequency and time. Figures 12(b) and 13(b) demonstrate the increase in variations in various frequency intervals (from 485 to 800 Hz for an eccentricity of 50 µm and reaching up to 1280 Hz for 100 µm). These fluctuations highlight the dynamic impact of eccentricity on the transmission error, an aspect that is less apparent in a frequency analysis. The 3D time-frequency results (Figures 14(b) and 14(c)) illustrate the energy changes and multiple harmonics created by eccentricity, showing how these disrupt the system dynamics.

The 3D Waterfall FFT demonstrates the progression of frequencies and amplitudes for time and speed. Figures 15(b) and 15(c) highlight transmission errors due to eccentricity through amplitude modulations and decreases, which would be difficult to detect with traditional FFT. These results make gears' complex and transient behavior tangible, considerably simplifying their interpretation. Therefore, traditional approaches documented in the literature (such as time and frequency domain analyses) usually focus on stable signals and simple anomalies. For instance, the cited sources [2-3] and [7] use theoretical models and FFT to analyze eccentricity but do not consider transient dynamics. However, this study uses methods designed explicitly for non-stationary signals, crucial for real-world systems where speed and load fluctuate.

The experimental data (Figures 11 to 15) demonstrate the effectiveness of these methods to facilitate the identification of anomalies that would otherwise remain invisible. These include the sidebands surrounding the meshing frequency (f_m), recurring discontinuities in the vibration signal, and, most importantly, fluctuations in the TE rate, as shown in Figure 16, which is an essential parameter for assessing the condition of the gears.

6. Conclusion

These techniques are particularly notable for their high sensitivity to eccentricity effects, especially for detecting transmission anomalies. Furthermore, the combined time-frequency approach (RPM frequency map, STFT, 3D waterfall FFT, and 3D Time-Frequency map) allowed for accurately capturing the nonlinear dynamic responses induced by these anomalies, providing a more detailed understanding of the system behaviour than traditional FFT techniques. These methods have proven exceptionally responsive to the effects caused by eccentricity, especially for detecting transmission irregularities. In addition, combined time-frequency techniques have highlighted the nonlinear dynamic reactions generated by these anomalies, thus providing a more comprehensive assessment of the overall system operation compared to conventional FFT methods. In the 2D dynamic transmission error spectrums, deviations from the expected values indicate the presence of vibrations. As misalignment and angular deviation intensify, the eccentricity increases from 0 to 100 µm, leading to a greater transmission error.

Compared with conventional FFT, this study's 3D FFT waterfall approach more effectively reveals hidden frequency modulations, thus enabling early fault diagnosis. This highlights the practicality of these techniques in real-world diagnostic applications. This study provides an opportunity to establish a more complete profile of the defect signature by combining various advanced time-frequency methods in a single experimental system.

The statistical analyses (ANOVA, correlation, and regression) quantitatively confirmed that eccentricity errors significantly modify vibration amplitudes ($p < 0.001$), while sideband energy ($r > 0.89$) shows a significant correlation ($r > 0.89$) with a negative correlation ($R2 = a$). These results support the diagnostic value of time-frequency measurement methods. Based on these results, integrating RPM frequency map, STFT, 3D waterfall FFT, and 3D Time-Frequency map into industrial machine condition monitoring systems could significantly reduce unexpected gearbox failures. The obtained results can significantly influence future research directions and practical applications in diagnostics.

Ethical and Data Integrity

No human subjects or animals were used to collect the data in this study, which was conducted under strictly controlled laboratory conditions. The authors attest to the utmost integrity in the recording, processing and reporting data.

Acknowledgments

The authors are grateful for the resources and equipment provided by the Department of Industrial Engineering, Operation Management, and Mechanical Engineering at Vaal University of Technology (South Africa) to enable this work.

References

[1] Olivier Petrilli et al., *Neural Network-Based Fault Detection Using Different Signal Processing Techniques as Pre-Processor*, ASME. New York, 1995. [Google Scholar] [Publisher Link]

[2] Wang Guangjian et al., "Research on the Dynamic Transmission Error of A Spur Gear Pair with Eccentricities by Finite Element Method," *Mechanism and Machine Theory*, vol. 109, pp. 1-13, 2017. [CrossRef] [Google Scholar] [Publisher Link]

[3] Xiuzhi He et al., "Effects of Gear Eccentricity on Time-Varying Mesh Stiffness and Dynamic Behavior of a Two-Stage Gear System," *Journal of Mechanical Science and Technology*, vol. 33, no. 3, pp. 1019-1032. [CrossRef] [Google Scholar] [Publisher Link]

[4] Zheng Cao et al., "Effects of the Gear Eccentricities on the Dynamic Performance of a Planetary Gear Set," *Nonlinear Dynamics*, vol. 20, no. 1, pp. 1-15, 2018. [CrossRef] [Google Scholar] [Publisher Link]

[5] Yong Yi et al., "Non-linear Dynamic Modelling, and Analysis for A Spur Gear System with Time-Varying Pressure Angle and Gear Backlash," *Mechanical Systems and Signal Processing*, vol. 132, pp. 18-34, 2019. [CrossRef] [Google Scholar] [Publisher Link]

[6] Fan Suxiang, and Hou Shulin, "Design and Application of the Eccentric Modified Gears," *1st International Conference on Mechanical Engineering and Material Science (MEMS 2012)*, Atlantis Press, 2012. [CrossRef] [Google Scholar] [Publisher Link]

[7] George W. Michalec, *Precision Gearing: Theory and Practice*, New York, Wiley, 1966. [Google Scholar]

[8] Cisheng Wu, "Transmission Error Caused by Gear Eccentricity Error," *Journal of Nanjing Institute of Technology*, vol. 12, no. 4, pp. 133-145, 1982. [Google Scholar]

[9] James R. Ottewill, Simon A. Neild, and R. Eddie Wilson, "Intermittent Gear Rattle due to Interactions between Forcing and Manufacturing Errors," *Journal of Sound and Vibration*, vol. 321, no. 3-5, pp. 913-935, 2009. [CrossRef] [Google Scholar] [Publisher Link]

[10] Ernesto Rocca, and Riccardo Russo, "Theoretical and Experimental Investigation into the Influence of the Periodic Backlash Fluctuations on the Gear Rattle," *Journal of Sound and Vibration*, vol. 330, no. 20, pp. 4738-4752, 2011. [CrossRef] [Google Scholar] [Publisher Link]

[11] Xiaoyu Gu, and Philippe Velex, "On the Dynamic Simulation of Eccentricity Errors in Planetary Gears," *Mechanism and Machine Theory*, Vol.61, pp. 14-29, 2013. [CrossRef] [Google Scholar] [Publisher Link]

[12] Aijun Hu et al., "Dynamic Modeling and Analysis of Multistage Planetary Gear System Considering Tooth Crack Fault," *Engineering Failure Analysis*, vol. 137, 2022. [CrossRef] [Google Scholar] [Publisher Link]

[13] Ning Liu et al., "Dynamic Characteristics of Gear-Rotor System with Gear Eccentricity and Wear Fault," *Nonlinear Dynamics*, vol. 112, pp. 16003-16035, 2024. [CrossRef] [Google Scholar] [Publisher Link]